White Rose Research Online

eprints@whiterose.ac.uk
https://eprints.whiterose.ac.uk
Universities of Leeds, Sheffield and York

Deposited via The University of Leeds.

White Rose Research Online URL for this paper:
https://eprints.whiterose.ac.uk/id/eprint/247105/

Version: Accepted Version

Article:
Kalybek, M., Bocian, M., Pakos, W. et al. (Accepted: 2026) Validation of vision-based vibration measurements for finite element modal updating of a cable-stayed bridge. Advances in Bridge Engineering. ISSN: 2662-5407 (In Press)

This is an author produced version of an article accepted for publication in Advances in Bridge Engineering (ABE), made available via the University of Leeds Research Outputs Policy under the terms of the Creative Commons Attribution License (CC-BY), which permits unrestricted use, distribution and reproduction in any medium, provided the original work is properly cited.

Reuse
This article is distributed under the terms of the Creative Commons Attribution (CC BY) licence. This licence allows you to distribute, remix, tweak, and build upon the work, even commercially, as long as you credit the authors for the original work. More information and the full terms of the licence here: https://creativecommons.org/licenses/

Takedown
If you consider content in White Rose Research Online to be in breach of UK law, please notify us by emailing eprints@whiterose.ac.uk including the URL of the record and the reason for the withdrawal request.

UNIVERSITY OF LEEDS
University of Sheffield
UNIVERSITY of York

Validation of vision-based vibration measurements for finite element modal updating of a cable-stayed bridge

Maksat Kalybek[1], Mateusz Bocian[2,*], Wojciech Pakos[3], Jacek Grosel[3], Nikolaos Nikitas[2]

[1]School of Information Technologies and Applied Mathematics, SDU University, 040900 Almaty, Kaskelen, 1/1 Abylaikhan Street, Kazakhstan

[2] School of Civil Engineering, University of Leeds, Woodhouse Lane, Woodhouse, Leeds LS2 9LG, United Kingdom

[3]Faculty of Civil Engineering, Wrocław University of Science and Technology, Wybrzeże Stanisława Wyspiańskiego 27, 50-370 Wrocław, Poland

* Corresponding author: M.Bocian@leeds.ac.uk

Abstract

This study presents a finite element (FE) model updating approach for a laboratory-scale cable-stayed bridge using vibration data obtained from a vision-based measurement system. Conventional accelerometer-based responses were used as a reference for comparison. The bridge's dynamic properties were extracted through experimental modal analysis under controlled excitation using both pseudo-random and sine-chirp signals. Optical motion tracking was performed using Template Matching (TM) and Optical Flow (OF) techniques, with the latter demonstrating superior accuracy and stability. A sensitivity-based, iterative Bayesian updating framework was employed to adjust key physical parameters, including the moduli of elasticity of the stay cables and stiffness at the deck supports. Results show excellent agreement between updated model predictions and experimental data, with modal frequency errors reduced from up to 16% to less than 1.5% and Modal Assurance Criterion (MAC) values exceeding 99%. The outcomes confirm that camera-based vibration monitoring can provide reliable data for FE model updating, achieving comparable accuracy to accelerometer-based methods while maintaining the advantages of non-contact and easily deployable measurements.

Keywords: optical motion-capture system, machine vision, structural vibrations, bridge engineering, modal analysis

1 Introduction

Finite Element (FE) models are fundamental tools in the analysis and design of civil engineering structures. They are extensively used for condition assessment, structural health monitoring (SHM), performance forecasting, and damage detection [1–3]. However, such numerical models are typically derived from idealised engineering blueprints and rely on uncertain assumptions regarding boundary conditions, geometry, and material properties [1,4–6]. Consequently, the predicted structural behaviour often diverges from the actual dynamic response of the as-built structures.

To bridge this gap, finite element model updating (FEMU) has emerged as an essential technique for enhancing the fidelity of numerical models through the incorporation of experimental data [4,7]. Conventionally, this process relies on the measurement of structural displacement under a prescribed static loading. In the context of structural dynamics, this process – often termed *finite element modal updating* – usually relies on vibration responses acquired from accelerometer-based monitoring systems to obtain information on natural frequencies and mode shapes. This approach has been successfully applied to a wide range of structures, including high-rise buildings [2,8], towers [5], full-scale bridges [9–12], scaled building models [13], and laboratory-scale bridge specimens [14].

Recent advances in computer vision technologies have introduced camera-based vibration monitoring as a promising alternative for modal analysis and SHM applications [15–17]. Vision-based systems, implemented via fixed cameras [16,18], unmanned aerial vehicles (UAVs) [19–21], or even smartphones [22,23], enable full-field, non-contact, and easily deployable measurements of structural motion. These methods have been successfully demonstrated in both experimental modal analysis (EMA), employing a known excitation force [24–26], and operational modal analysis (OMA), relying on ambient conditions to provide an unknown excitation force to the structure [27,28]. As vision-based sensing matures, increasing attention has turned towards its use in higher-level tasks such as FE model updating, damage detection, and performance forecasting [29,30].

Despite these advances, existing studies have predominantly focused on the direct FE model updating methods in which modifications are introduced directly to the stiffness and mass matrices. However, this often comes

at the cost of lost interpretability, as linking these changes to tangible material or geometric properties can be difficult [3,31]. In contrast, iterative FE model updating methods, in which modifications are introduced to the physically meaningful model parameters such as stiffness, mass density, or boundary conditions, preserve the model's realism and diagnostic value. Updating actual physical parameters not only enhances predictive performance but also allows independent validation against measurable structural properties. To the authors' knowledge, vision-based FE model updating targeting physically interpretable parameters, rather than just numerical stiffness and mass matrices, has not yet been comprehensively explored.

Iterative finite element (FE) model updating is generally based on sensitivity analysis, which quantifies how variations in model parameters influence structural responses such as natural frequencies and mode shapes. In this context, the parameters represent uncertain structural properties of the numerical model, including boundary conditions, stiffness, material density, and cross-sectional properties, while the responses correspond to modal characteristics obtained from either experimental measurements or FE analysis. The sensitivity matrix is used to describe the relationship between parameter variations and response changes and can be calculated numerically using approaches such as the forward finite difference method [4].

A critical step in the updating process is the selection of parameters to be modified. To avoid non-unique or physically unrealistic solutions, only parameters that are both uncertain and highly influential on the selected responses are typically considered. During each iteration, the sensitivity matrix is recalculated based on the updated parameter values. Using a first-order Taylor series approximation, the differences between experimental and analytical responses are related to the corresponding parameter corrections, allowing the model to be progressively refined until the discrepancies between measured and predicted responses satisfy predefined convergence criteria.

The model updating procedure adopted in the present study follows a Bayesian-based updating framework. In this approach, the parameter correction vector is obtained by minimizing an objective function that simultaneously reduces the discrepancy between experimental and numerical modal responses while limiting deviations from the initial parameter estimates. Weighting matrices are assigned to both the response residuals

and the parameter variations to represent the confidence placed in the measured data and the prior model assumptions, respectively [32].

This Bayesian-based formulation provides a balanced updating strategy that improves numerical stability, promotes convergence, and prevents unrealistic parameter modifications, particularly when the available experimental data are limited. The weighting factors are incorporated into a gain matrix that determines the parameter adjustments required at each iteration, ensuring that the updated model remains both mathematically stable and physically meaningful.

Consequently, the overall FE model updating procedure consists of three principal stages:

1. Selection of target modal responses, such as experimentally identified natural frequencies and mode shapes.
2. Sensitivity analysis to identify uncertain model parameters that significantly influence the selected responses.
3. Iterative updating of the selected parameters using the Bayesian-based updating framework until the specified convergence criteria are satisfied

While the ultimate goal of FEMU is the calibration of FE models of full-scale, in-situ structures, laboratory studies offer critical advantages by eliminating uncontrolled environmental and operational influences. As such, they enable a systematic evaluation of emerging sensing and FEMU methodologies. To this end, the present study aims to advance the application of vision-based vibration monitoring to FE modal updating by demonstrating its effectiveness in the case of a scaled model of a cable-stayed bridge set in a controlled laboratory environment. The dynamic characteristics of the structure, i.e. natural frequencies and mode shapes [25] are obtained through EMA using a shaker as an excitation source. The updated model derived from vision-based data is validated against results obtained from conventional accelerometry to assess its reliability and accuracy.

The remainder of this paper is organised as follows. Section 2 presents the materials and methods, including the description of the tested structure and the development of the initial FE model. Experimental setup is then

presented, focusing on the camera-based motion tracking systems and data analysis, including the modal identification procedures. Section 3 outlines the FE model updating methodology, including the sensitivity analysis and parameter selection process, and the model updating procedure. The findings from the modal updating study are discussed in Section 4. Section 5 concludes the paper with a summary of key outcomes and recommendations for future work.

2 Materials and methods

2.1 Tested structure

The laboratory model of the cable-stayed bridge and the configuration of the instrumentation are illustrated in Figure 1. The bridge's geometry and dynamic behaviour were designed to replicate, at scale, the characteristics of full-size cable-stayed bridges. The structure features two spans: a main span of 4550 mm and a shorter span of 1550 mm, with the outermost supports positioned 50 mm inward from the deck edges. The pylon rises 2880 mm and comprises two legs joined by a cross-beam, with each leg fitted with a cable anchorage plate at the top. The short span includes an auxiliary support that permits longitudinal displacement. The deck, constructed from a 15 mm thick and 250 mm wide solid steel plate, is supported 595 mm above the ground. Four pairs of stay cables connect the main span to the pylon, while two additional pairs comprise the back-stays. All supports are made of a stiffened steel beam bolted to the strong floor. The deck is restrained against longitudinal motion at the pylon but remains free to rotate, and longitudinal translation is allowed at all other supports. Overall, the bridge exhibits low-frequency vibration modes with low damping. More detailed description of the bridge can be found in [33].

(a) (b)

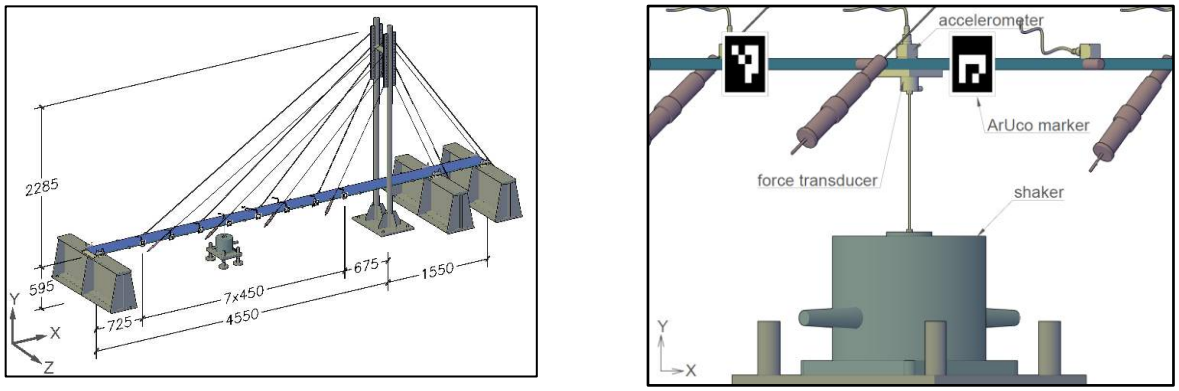


Figure 1. Layout of the bridge model and instrumentation system: (a) overview of the bridge; (b) zoomed-in view of the bridge deck section near the shaker attachment point. All dimensions are given in millimeters.

2.2 Initial FE model

An FE model of the bridge, shown in Figure 2, was developed in SAP2000 v20 [34], a popular software used for structural analysis. The deck and pylon were modelled using three-dimensional frame elements with section properties corresponding to the geometry of the laboratory structure. The deck was represented by a rectangular steel section corresponding to the 250 mm × 15 mm steel plate described in Section 2.1, while the pylon members were represented by circular hollow steel sections. The stay cables were modelled using SAP2000 cable elements, i.e. tension-only nonlinear catenary elements capable of representing cable sag effects and the associated geometric nonlinearity. The connection between the deck and the pylon was modelled using a link element.

The model discretisation was defined by placing nodes at support locations, cable anchorage points, and measurement locations used in the experimental campaign. This facilitated direct comparison between the numerical and experimental modal responses. Automatic meshing was then employed to ensure compatibility between the deck, pylon, and cable elements. As no direct measurements were available prior to the experimental campaign, the initial post-tensioning forces in the stay cables were estimated based on values reported in previous studies on the same bridge [35], as illustrated in Table 3. The deck was assumed to be restrained against translational movement at the pylon (support ② in Figure 3) while remaining free to rotate. At all the other supports (supports ①, ③, ④ in Figure 3), the deck was free to translate along the longitudinal axis of the deck and free to rotate.

A non-linear static analysis under self-weight was first carried out in SAP2000 to capture the geometric non-linearity introduced by cable sag. This step established the correct pre-deformed configuration and the corresponding cable tension state. A modal analysis was then performed using the stiffness matrix obtained at the end of this non-linear load case. This sequential procedure, i.e. non-linear static analysis followed by linear dynamic analysis using the updated stiffness, is widely applied in cable-stayed bridge modelling and has been shown to yield more accurate natural frequencies and mode shapes [11,36].

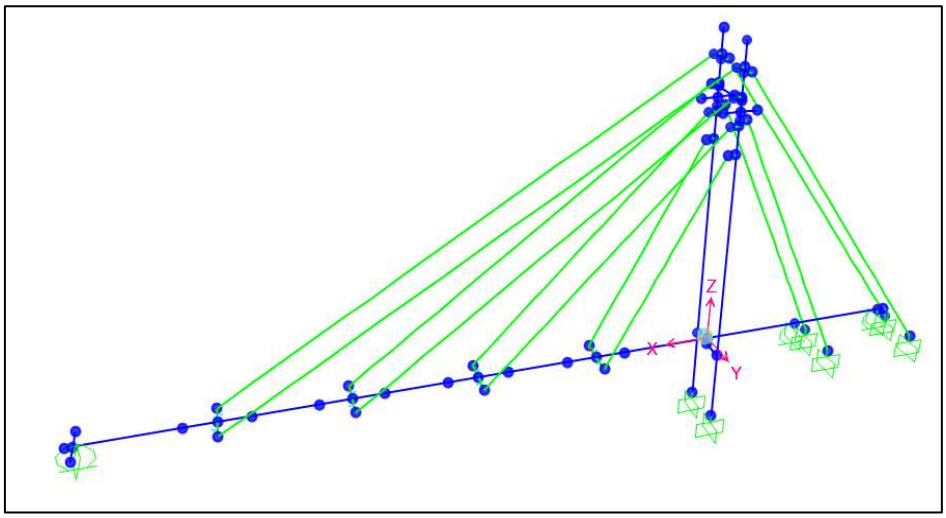


Figure 2. Initial FE model of the bridge.

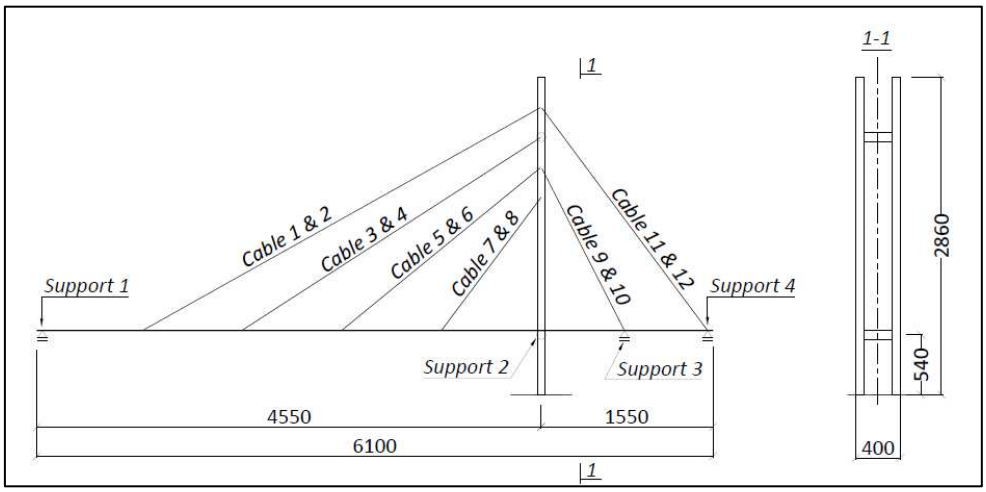


Figure 3. Basic bridge dimensions and springs used to model the support conditions.

2.3 Experimental setup

The experimental setup and procedures were extensively described in the authors' earlier publication [25]. Therefore, only a brief description is provided herein to give a context to the FE model updating.

Experimental modal analysis was performed using shaker excitation and structural responses of the deck were measured by both conventional accelerometery and a camera-based optical motion capture system (MCS). Four forced vibration tests (T1–T4) were carried out using two types of excitation signals, namely pseudo-random and sine chirp, each type applied at two intensity levels, as show in Table 1. Structural response data were extracted from the video recordings using two motion-tracking algorithms implemented in a custom C++ software package. Each test lasted approximately 10 minutes, and the complete measurement campaign was completed within three hours in a stable indoor laboratory environment. The controlled testing conditions and consistent measurement durations contributed to signal stability and repeatability. Optical markers were positioned at the same locations as the accelerometers along the deck, enabling direct spatial correlation between the two datasets. The extracted modal parameters were subsequently compared for validation and analysis.

Table 1. Summary of the conducted forced vibration tests.

Test ID	Excitation type	Rate [Hz/s]	RMS intensity [N]	Test duration [s]	Frequency range [Hz]
T1	pseudo-random	n/a	13.35	600	3–25
T2	pseudo-random	n/a	28.95	600	3–25
T3	sine chirp	0.037	9.69	600	3–25
T4	sine chirp	0.037	19.8	600	3–25

2.3.1 Vibration exciter and accelerometers

Dynamic structural excitation was applied using Brüel & Kjær Type 4808 permanent magnetic shaker (force rating: 112 N), mounted on a rigid steel plate anchored to the laboratory strong floor. The excitation force was transmitted to the deck via a stinger connected through a DeltaTron® 8320-003 force transducer. The excitation point was 2.075 m away from the furthest deck support from the pylon and centred transversely.

Input signals were generated using Brüel & Kjær's PULSE DAQ system operating at 24-bit resolution and a sampling rate of 4096 Hz.

The bridge response was recorded using ten Brüel & Kjær miniature DeltaTron® 4507 B005 accelerometers. Seven accelerometers were mounted along the edge of the main span of the bridge facing the camera, adjacent to the ArUco markers, while two additional accelerometers were installed on the opposite side to capture horizontal and torsional vibration modes. An extra accelerometer was collocated with the force transducer to obtain the driving point frequency response functions and to scale the mode shapes.

2.3.2 Optical motion capture system

The optical system consisted of a Canon EOS 200D camera with a DIGIC 7 processor and a 20 mm lens. A set of ArUco fiducial markers was used for motion tracking, each marker measuring 100 × 100 mm (including a white border) and printed on laminated polystyrene foam boards. The marker dimensions and camera-to-structure distance were selected following the methodology proposed by Kalybek et al. [24], which systematically evaluated the influence of marker size, camera distance, and viewing angle on the accuracy of ArUco-based pose estimation. The markers were mounted along the deck at 450 mm intervals using hot melt glue. The short span of the bridge was not instrumented due to its higher stiffness and limited contribution to the modes of interest. The camera was positioned 5 meters from the structure at deck level to minimize angular distortion, with the incidence angle kept below three degrees across the long span. Video recordings were captured at 59.94 frames per second (fps) with fixed focus and exposure settings to maintain consistency.

The purpose of the image-processing procedure was to extract two-dimensional structural displacement time histories from the recorded videos. This was achieved using established computer vision techniques rather than by modifying the underlying tracking algorithms themselves. Two motion capture algorithms were used: template matching (TM) and optical flow (OF). In both cases, the processing included camera calibration and lens distortion correction, definition of regions of interest around the tracked markers, localisation of marker or feature positions in the image plane, sub-pixel refinement, and transformation of image coordinates into physical displacement coordinates using homography. The resulting displacement time histories were then

used for modal identification and subsequent FE model updating. The theoretical background and the image processing workflow applied in this study are outlined in the following sections.

2.3.2.1 Template matching

Area-based template matching (TM) is a widely used motion capture algorithm that operates by sliding a predefined image, known as the template, across a larger image to identify the region of the best correspondence. Matching is typically achieved using the correlation or difference-based methods [37], with the normalised correlation coefficient being particularly common due to its robustness against lighting variations. TM has been extensively applied in structural monitoring of bridges [14,38,39], towers, and laboratory-scale models[40], owning to its simplicity and capability for fully contactless measurements with minimal user input [41,42].

The TM system used in this study was custom-developed to track multiple targets on the structure. The technique works by comparing each frame of the recorded video to a reference image selected at the beginning of testing. The algorithm searches within a user-defined search window to locate the region that most closely resembles the reference ROI. This improves both efficiency and accuracy by limiting the search area. Although the laboratory environment provided relatively stable lighting conditions during the experimental campaign, minor variations in ambient illumination were unavoidable. Therefore, the normalised correlation coefficient was used as the matching criterion, as it has been demonstrated to be more robust to changes in lighting intensity than alternative correlation measures [43]. Once the closest match is found, its pixel coordinates are refined to subpixel accuracy using enhanced cross-correlation (ECC) interpolation. The final step is transforming these tracked pixel coordinates into real-world displacements. This is achieved by applying a projective transformation matrix obtained from the known correspondence between image and physical coordinates using homography, and correcting for camera lens distortion using calibration data.

The flowchart for TM motion tracking is presented in Figure 4.

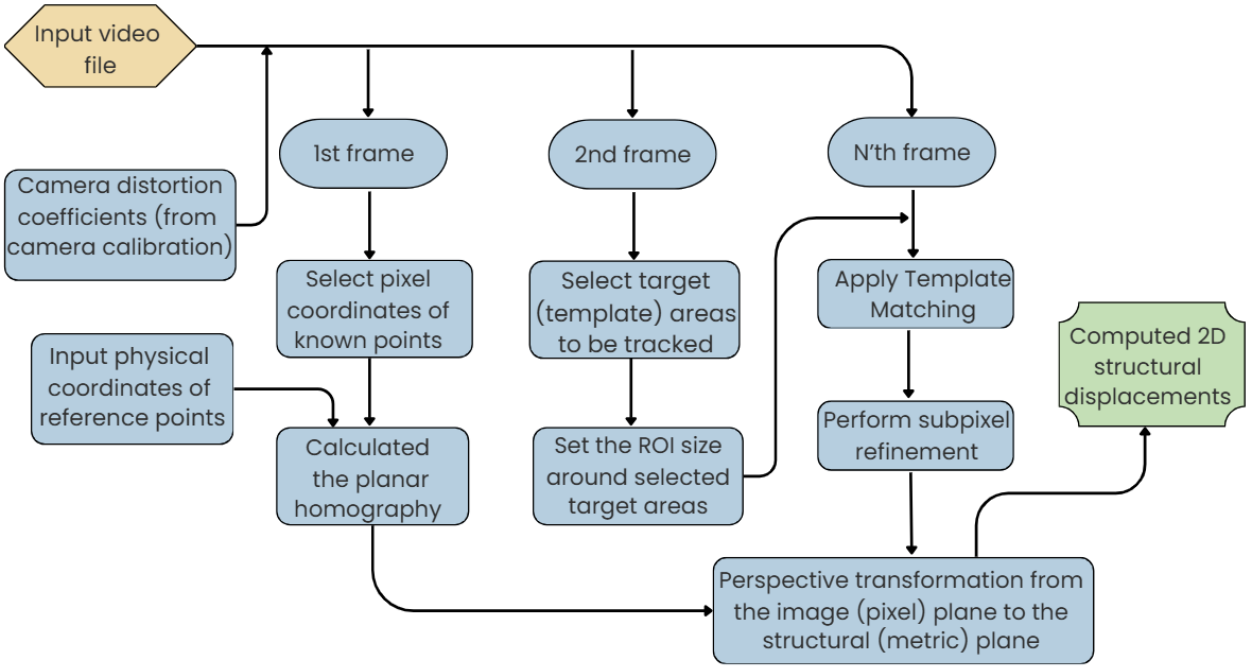


Figure 4. Flowchart illustrating the procedure adopted for motion tracking using the Template Matching (TM) algorithm.

2.3.2.2 Optical flow method

Optical flow (OF) is an image processing technique widely applied in SHM [44]. The method estimates motion by tracking feature points – typically corners or edges, between consecutive video frames. It relies on several key assumptions: the brightness of individual points remains constant over time, inter-frame motion is relatively small, and neighbouring points move coherently.

In sparse OF methods, such as the Lucas–Kanade algorithm [45] employed in this study, motion is computed only for distinctive points within selected ROIs, rather than across the entire image. Therefore, specific ROIs were defined within the first video frame. Within these ROIs, distinctive corner-like features were identified in the reference frame using the Shi–Tomasi corner detection method [46]. Once detected, the motion of these features was continuously tracked across subsequent frames by estimating their positional changes over time. Instead of referencing the initial frame throughout, the system updated its reference at each step based on the most recently tracked frame, thereby improving robustness against gradual lighting variations, minor scale changes, and feature loss or drift. For each ROI, the tracked feature coordinates were averaged to obtain representative motion values. These pixel displacements were then converted to physical displacements using

the same camera calibration and transformation procedures as those applied in the TM system described in Section 2.3.2.1.

The flowchart for OF motion tracking is presented in Figure 5.

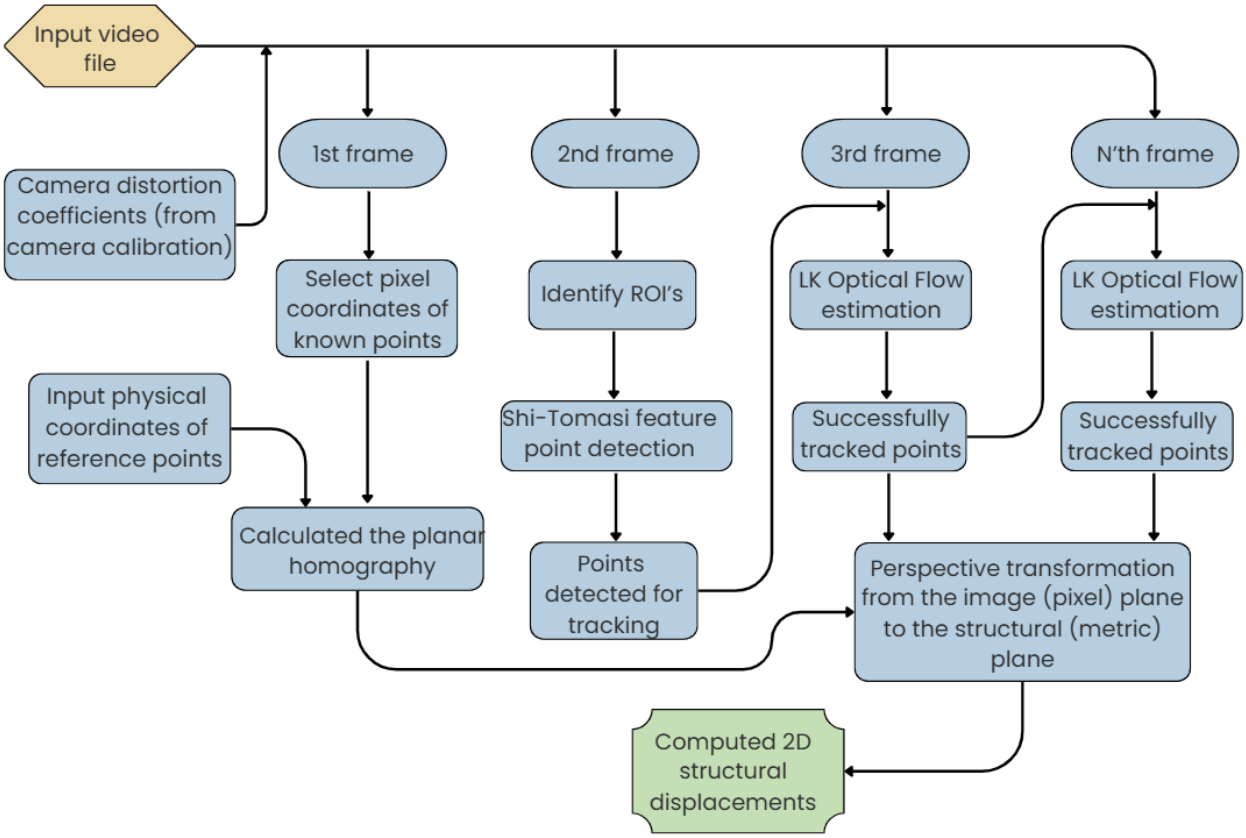


Figure 5. Flowchart illustrating the procedure adopted for motion tracking using the Optical Flow (OF) algorithm.

2.3.3 Data processing and modal analysis

The data processing workflow consisted of three main stages: signal resampling, time alignment, and modal analysis. All sensor data, including those from the camera, accelerometers, and force transducers, were first resampled to a common frequency of 333 Hz to ensure precise temporal synchronization. MATLAB's *resample* function, incorporating finite impulse response (FIR) filtering, was used to preserve signal fidelity during this process. Time alignment between measurement systems was achieved by matching acceleration and displacement signals at the excitation point using a least-squares fitting approach. Prior to alignment, the

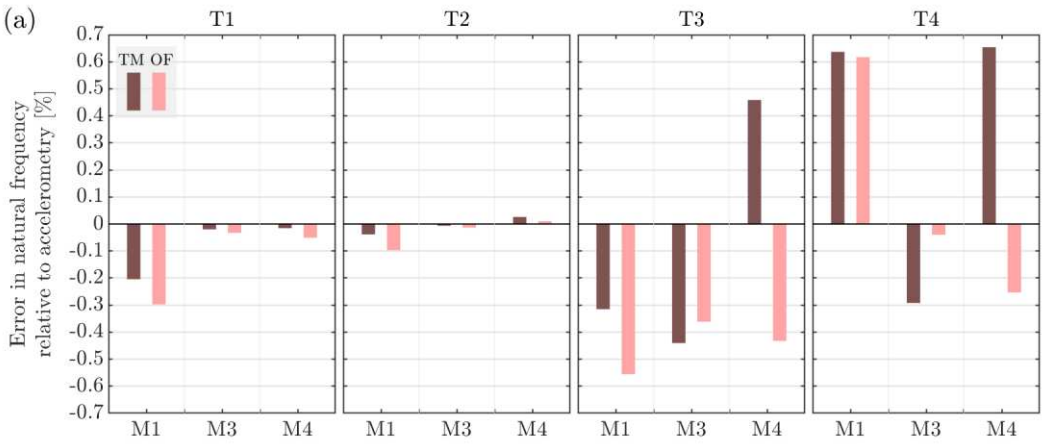
signals were band-pass filtered, and single-order integration or differentiation was applied as required to obtain velocity signals.

Subsequent modal analysis was performed using the PolyMAX™ algorithm implemented in Siemens TestLab. This algorithm estimates frequency response functions (FRFs) via a poly-reference least-squares method in the frequency domain. Both H_1 and H_2 estimators were evaluated, however, the H_1 estimator was selected for its superior performance under low-noise input conditions. Additional signal processing steps, including windowing and truncation, were applied as appropriate to the excitation type (pseudo-random or sine chirp) to minimize spectral leakage and transient effects.

3 Results

3.1 Identification of modal characteristics

The results of the modal analysis are summarized in Table 2. Across all tests, three dominant modes were consistently identified: two primarily associated with deck bending (modes 1 and 4) and one dominated by the pylon's motion (mode 3), as will be shown when discussing the performance of FE models (see Figure 13). Another vibration mode was also apparent in the measured signals, however, it was not explicitly identified because the excitation force was applied at a node corresponding to that mode. The errors in the identification of modal frequency, damping and generalised mass, relative to the results from accelerometry, for each of these modes are visualised in Figure 6.



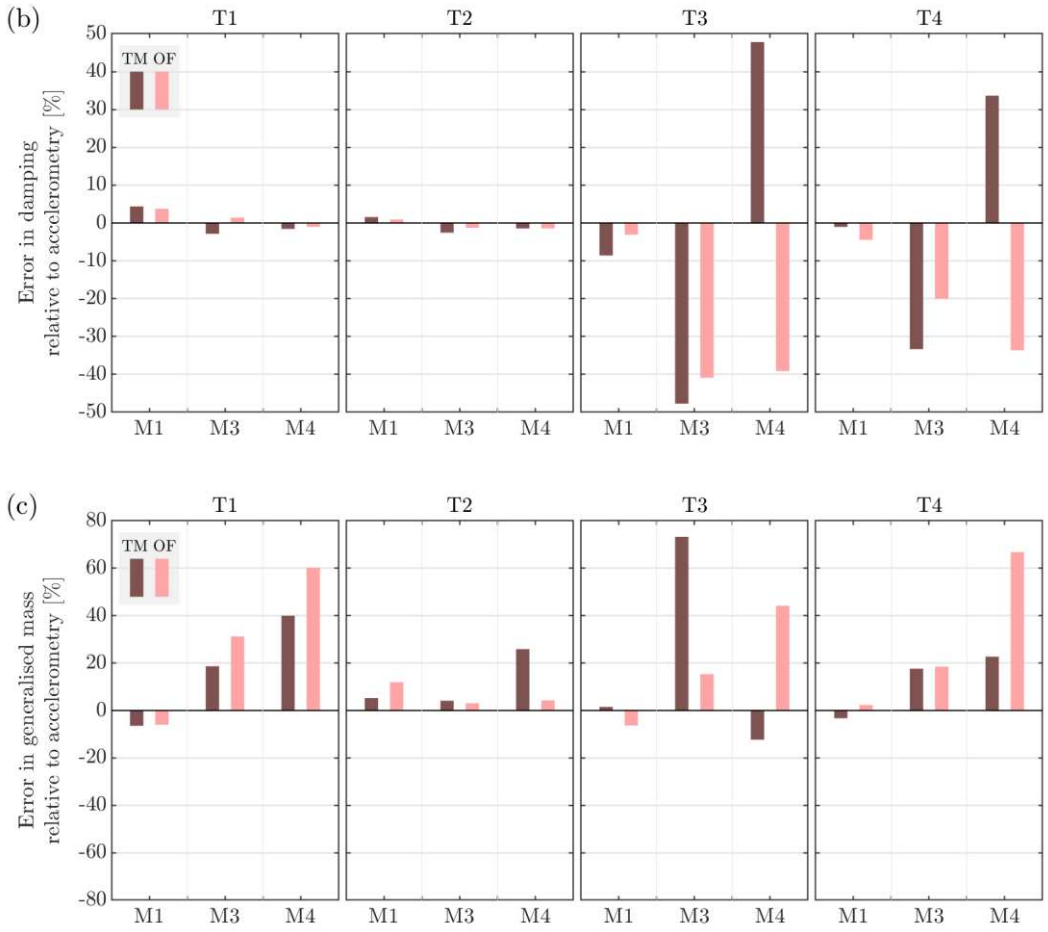


Figure 6. Percentage error in the (a) natural frequency, (b) modal damping, and (c) generalised mass based on data extracted using template matching (TM) and optical flow (OF) algorithms relative to the results obtained from accelerometry for the four tests specified in Table 1 (T1 – T4) and modes 1, 3 and 4 (M1, M3 and M4, respectively).

The accuracy of the identified modal parameters was found to depend strongly on the type of excitation and its intensity. As can be seen in Figure 6, pseudo-random excitation yielded more accurate and stable results in terms of modal frequency and damping identification than sine chirp excitation. This effect was most evident in T2, which used higher-intensity pseudo-random excitation and produced the closest agreement between optical and accelerometer-based measurements. In this case the errors in modal frequencies for all modes were negligible, i.e. below 0.1%, and MAC values between optical and accelerometer mode shapes exceeded 0.95, indicating excellent correlation. The error in the damping ratio was below 2.6%. Although the error in identifying the generalised mass was typically the highest of all the dynamic characteristics, T2 still yielded the least variability across all tests.

Table 2. Modal properties of the bridge. The values in brackets indicate the percentage error relative to the corresponding results obtained from accelerometry.

		Frequency [Hz]			Damping ratio [%]			Generalised mass [kg]		
Test ID	**Mode #**	**ACC**	**TM**	**OF**	**ACC**	**TM**	**OF**	**ACC**	**TM**	**OF**
T1	1	5.384	5.373 (−0.2)	5.368 (−0.3)	4.79	5.00 (4.38)	4.97 (3.76)	89.5	83.7 (−6.45)	84.1 (−6.01)
T1	3	15.218	15.215 (−0.02)	15.213 (−0.03)	0.70	0.68 (−2.86)	0.71 (1.43)	353.0	418.9 (18.67)	463.3 (31.24)
T1	4	19.637	19.634 (−0.02)	19.627 (−0.05)	1.91	1.88 (−1.57)	1.89 (−1.05)	79.8	111.7 (39.91)	127.9 (60.24)
T2	1	5.182	5.180 (−0.04)	5.177 (−0.1)	3.19	3.24 (1.57)	3.22 (0.94)	87.8	92.4 (5.2)	98.3 (11.85)
T2	3	15.082	15.081 (−0.01)	15.08 (−0.01)	0.78	0.76 (−2.56)	0.77 (−1.28)	371.9	387.3 (4.14)	383.3 (3.06)
T2	4	19.178	19.183 (0.03)	19.18 (0.01)	2.09	2.06 (−1.44)	2.06 (−1.44)	80.7	101.6 (25.97)	84.13 (4.3)
T3	1	5.398	5.381 (−0.31)	5.368 (−0.56)	2.91	2.66 (−8.59)	2.82 (−3.09)	110.8	112.5 (1.51)	103.8 (−6.34)
T3	3	15.210	15.143 (−0.44)	15.155 (−0.36)	0.88	0.46 (−47.73)	0.52 (−40.91)	369.7	640.5 (73.22)	426.5 (15.35)
T3	4	19.410	19.499 (0.46)	19.326 (0.43)	1.15	1.70 (47.83)	0.70 (−39.13)	119.2	104.5 (−12.36)	171.9 (44.2)
T4	1	5.182	5.215 (0.64)	5.214 (0.62)	2.92	2.89 (−1.03)	2.79 (−4.45)	94.0	90.9 (−3.21)	96.2 (2.4)
T4	3	15.059	15.015 (−0.29)	15.053 (−0.04)	0.90	0.60 (−33.33)	0.72 (−20)	396.3	466.2 (17.63)	469.6 (18.47)
T4	4	18.960	19.084 (0.65)	18.912 (−0.25)	1.07	1.43 (33.64)	0.71 (−33.64)	109.2	134.0 (22.71)	182.2 (66.85)

Of the two optical motion tracking methods, OF consistently outperformed TM, providing a more accurate identification of natural frequencies, damping and generalised masses. Combining OF with structural excitation during T2 yielded the most coherent and stable set of modal parameters. For this reason, the OF data from T2 were selected for subsequent FEMU comparative analysis with accelerometer-based results.

3.2 FE model updating

This section presents FE model updating study of a laboratory-scale cable-stayed bridge model based on the measured dynamic responses obtained via accelerometry and OF during T2. Section 3.2.1 presents a sensitivity analysis undertaken to determine the parameters for FE modal updating and the target responses used to evaluate FE models. Section 3.2.2 presents the rationale behind the adopted two-stage FE model updating strategy. Section 3.2.3 presents the fidelity of the FE models developed through the modal updating procedure.

3.2.1 FE model sensitivity analysis

FE model sensitivity analysis involves determining the candidate model parameters to be adjusted during the updating process and the target responses against which the models will be calibrated. These steps are described in Section 3.2.1.1 and Section 3.2.1.2, respectively. Section 3.2.1.3 then presents an FE model, used

296 in the updating process, having a reduced number of parameters that were found to significantly affect its
297 behaviour.

298 **3.2.1.1 Determination of parameters for FEMU**

299 FE model updating based on too many parameters, or parameters which do not significantly influence the
300 structural behaviour, may result in models that are physically unrealistic [4]. Therefore, the selection process
301 of model parameters chosen for updating should focus on those parameters that are uncertain and have the
302 greatest impact on the structural behaviour.

303 Boundary conditions at the deck supports were identified as key uncertain parameters. Initially, springs k_Δ and
304 k_ϕ were introduced at deck supports within the SAP2000 FE model to represent uncertain longitudinal and
305 rotational stiffnesses, respectively. To estimate the initial stiffness values of these springs, a preliminary static
306 analysis was carried out using the structure's self-weight, assuming fixed boundary conditions at all degrees of
307 freedom [4]. The resultant maximum reaction forces and moments provided baseline stiffness values; for
308 instance, initial longitudinal stiffness values ranged from 1.2×10^5 N/m to 6×10^5 N/m, and rotational stiffness
309 values were around 120 Nm/rad (Table 4). The initial model frequencies and Modal Assurance Criterion
310 (MAC) values obtained with these springs are detailed in Table 5 and Table 6, showing frequency
311 discrepancies reaching approximately 16%.

312 Previous studies [33,47] assumed a Young's modulus of 140 GPa for all cables on both sides of the pylon,
313 with differentiation only in the cross-sectional areas: 1.2 mm² for the cables on the longer deck span and
314 1.8 mm² for those on the shorter span. However, detailed information on the cable composition was not
315 available. Manufacturer guidelines [48] indicate that, for cables with steel cores, the elastic modulus may be
316 underestimated by approximately 25%. Given this uncertainty and considering that earlier studies may have
317 adopted a conservative lower-bound value of 140 GPa, the elastic moduli for the cables on the left (longer-
318 span) side of the deck ($E_{1\text{-}8}$) and those on the right (shorter-span) side ($E_{9\text{-}12}$) were explicitly treated as uncertain
319 parameters.

320 Additionally, cable post-tension forces (F_1 to F_{12}) were treated as uncertain, with initial values (i.e. forces
321 required to bring the deck level to horizontal, but without accounting for the forces developed in the cables

due to self-weight of the deck) ranging between 16.3 N and 563.6 N, as adopted from earlier study on the bridge (Table 3) [35], since explicit measurements before testing were unavailable. Thus, the parameters identified for updating included:

- Moduli of elasticity for stay cables ($E_{1\text{-}8}$ *and* $E_{9\text{-}12}$);
- Tension forces in twelve cables (F_1 to F_{12});
- Deck supports' translational (k_Δ; in longitudinal direction of the deck only) and rotational (k_ϕ) spring stiffnesses.

3.2.1.2 Target responses for FEMU

The SAP2000 Open Application Programming Interface (OAPI) was employed to facilitate seamless two-way data communication between SAP2000 and FEMTools [49], enabling a coordinated model updating process. While all FE analyses were executed within SAP2000, FEMTools served as the supervisory platform to orchestrate model updating tasks [50].

The target responses selected for model updating were natural frequencies and Modal Assurance Criterion (MAC) values of modes 1, 3, and 4, as reported in Section 2.4. Due to lower inherent reliability, MAC values were assigned confidence factors ten times lower than those for natural frequencies, aligning with best practices outlined by [36,51]. The FEM updating approach was based on Bayesian algorithms.

Initial correlations between the FE model parameters and measured modal responses (accelerometry and OF) are documented in Table 5 and Table 6. Notably, mode 3 exhibited the largest initial discrepancy (~16%) in frequency between measurements and FE predictions. Despite frequency differences, the mode shapes demonstrated good initial agreement, with minimum MAC values of 91.0% and 89.1% for accelerometry and OF, respectively.

3.2.1.3 Initial sensitivity analysis

A preliminary sensitivity analysis involved all 21 parameters described above to identify those parameters most influential on modal responses. Initially, measured modes were paired with FE modes using FEMTools'

automated pairing algorithm [49]. Sensitivity analysis subsequently quantified each parameter's impact on modal frequencies and MAC values.

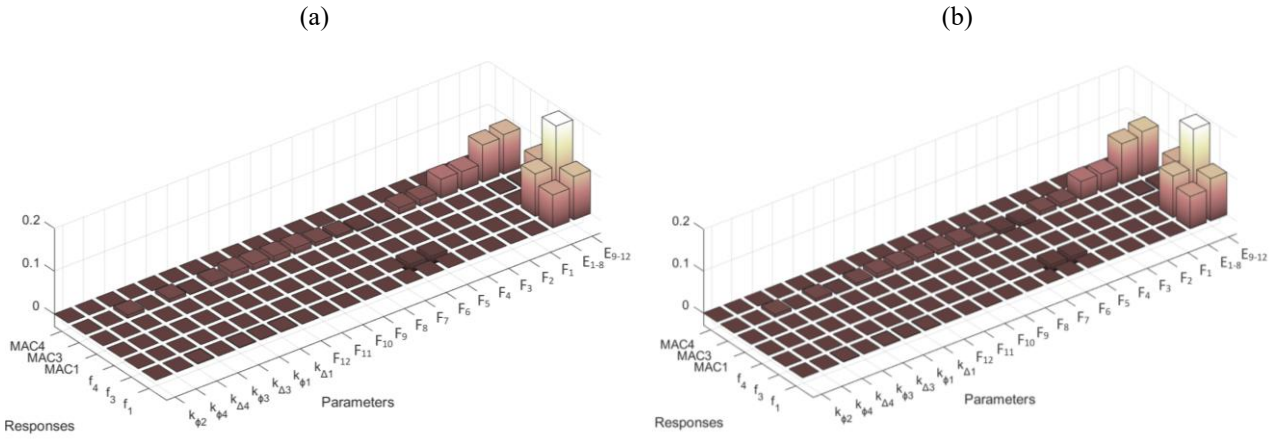


Figure 7. Normalised (i.e. unitless) sensitivity values of the target FE responses based on corresponding measurements from (a) accelerometry and (b) OF made during T2.

The results of the initial sensitivity analysis, presented in Figure 7, indicated that cable moduli of elasticity predominantly influenced the FE model, particularly affecting frequencies across all modes and MAC values for modes 1 and 4. These parameters consistently showed significantly higher sensitivity compared to other parameters, emphasizing their importance in subsequent updating procedures.

3.2.2 FE model updating strategy

Considering the results of the sensitivity analysis presented in Section 3.2.1, FEMU was conducted in two stages, outlined in detail in Section 3.2.2.1 & Section 3.2.2.2.

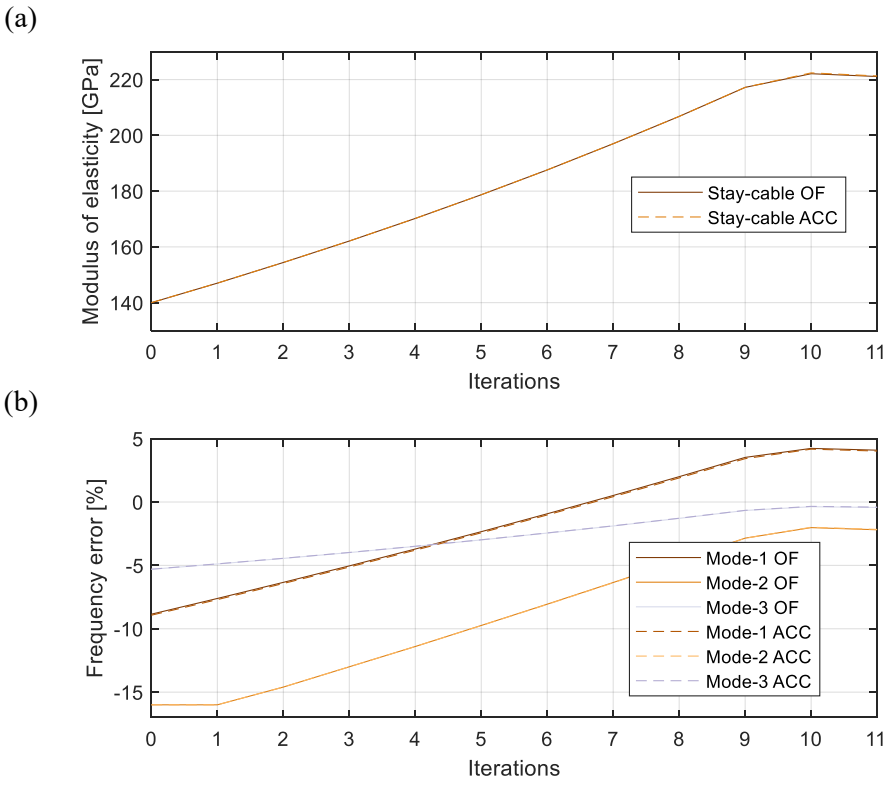
- Stage 1: The FE model was updated by adjusting the most sensitive parameters, specifically the moduli of elasticity for the stay cables, $E_{1\text{-}8}$ and $E_{9\text{-}12}$.
- Stage 2: After addressing cable moduli of elasticity, additional sensitivity evaluations guided further updates focused on deck support stiffness parameters, refining both translational (k_Δ) and rotational (k_ϕ) stiffness values.

3.2.2.1 Stage 1: stay cables' moduli of elasticity

The modal updating was conducted with stay cables' moduli of elasticity selected as the parameters to update. The "parameter relations" feature in FEMTools was applied to $E_{1\text{-}8}$ and $E_{9\text{-}12}$ to ensure consistency across all

365 cables, as their only difference lies in cross-sectional area, as discussed in Section 2.5.1.1. A limit of 5%
366 maximum change per iteration was imposed on parameter adjustments.

367 As shown in Figure 8, the difference between the results obtained using accelerometry and OF are
368 unnoticeable. After 11 iterations, the cable modulus converged to approximately 221 GPa. However, it was
369 observed that the first modal frequency, typically the most reliable due to ease of identification, began to
370 deviate after the sixth iteration. Linear interpolation indicated that the lowest error for this mode occurred when
371 $E_{1\text{-}8}$ and $E_{9\text{-}12}$ were approximately 188 GPa.



372

373 Figure 8. Updating process of stay cables' modulus of elasticity: (a) iterative change of the stay cable
374 modulus of elasticity, and (b) corresponding change in modal frequencies.

375 The final updated value of 221 GPa was deemed unrealistic, given the manufacturer's specifications and the
376 known uncertainty regarding cable composition. Consequently, an informed decision was made to adopt a
377 value of 175 GPa, consistent with manufacturer data for steel-core cables. This adjustment resulted in
378 substantial improvements in both modal frequencies and MAC values relative to the initial model, as reported
379 in the fourth column of Table 5 and Table 6 for accelerometry and OF, respectively.

3.2.2.2 Stage 2: update the deck's boundary conditions

Following the update of the governing parameter, the stay cables' modulus of elasticity, a sensitivity analysis was re-run for all remaining, less sensitives parameters. While Figure 9 demonstrates the target response sensitivities paired with the OF measurements, the model paired to acceleration measurements resulted in nearly identical results. The FEM exhibited the highest sensitivity to changes in the stiffness of the three translational springs at the supports away from the pylon (k_{Δ}) and the rotational spring at the furthest support from the pylon ($k_{\phi 1}$). In contrast, variations in the tensile forces within the cables did not show significant effect on the model response.

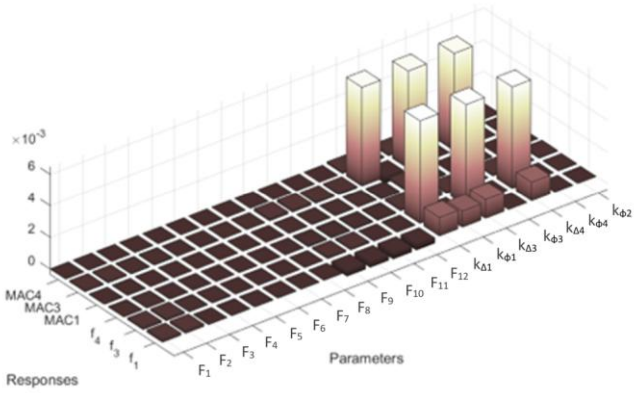


Figure 9. Normalised (unitless) sensitivity values of the target FE responses, paired with corresponding OF measurements, to variations in cable post-tension forces and support spring stiffnesses.

Given these findings, a model updating procedure was conducted using FEMTools, targeting the four most sensitive parameters. The process converged after 13 iterations, yielding a noticeable improvement in both natural frequencies and Modal Assurance Criterion (MAC) values. The average frequency discrepancy between the FE model and experimental data was reduced by 4.37%, with mode 3 showing the largest residual error.

Despite the substantial improvement, an alternative approach was explored to refine the assessment of the spring stiffness values and achieve better alignment between the FE model and experimental observations. This decision was motivated by the following rationale:

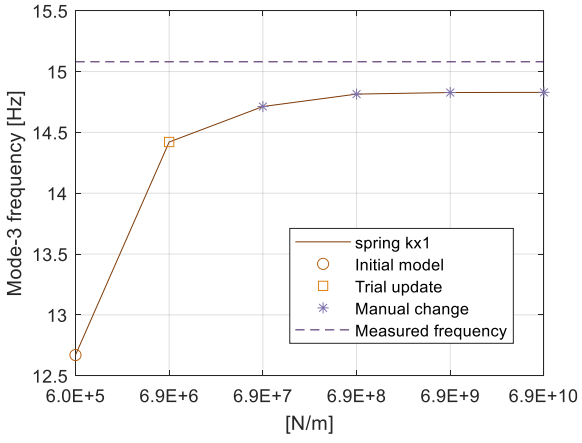
Based on previous studies [11,52], and observations of the deck-support interface, the supports were assumed to possess a degree of elasticity, represented by linear springs. While it is likely that the support at the pylon

400 could be idealised as a rotational spring, the mechanical behaviour of the supports located further from the
401 pylon remained uncertain. An example of such a support, situated at the furthest point from the pylon, is
402 illustrated in Figure 9. In this configuration, the deck is pressed against a roller (circular rod), whose movement
403 is restricted by L-shaped cross-beams and a set of springs.

404 Preliminary manual tests, in which the spring stiffness values were adjusted incrementally, demonstrated that
405 further improvements in modal response were achievable. For instance, Figure 10 shows that the frequency of
406 mode 3 aligns more closely with experimental data when the stiffness of the spring at the first support, $k_{\Delta 1}$, is
407 manually increased beyond the value obtained through automated model updating. However, this improvement
408 plateaus once the correlation reaches a threshold, indicating a reduced sensitivity of the model to additional
409 increases in this parameter beyond 6.9×10^8 N/m.



410 Figure 10. Arrangement of the bridge's bearing furthermost away from the pylon (first support).



411

412 Figure 11. Mode 3 frequency change achieved by altering the spring stiffness at the first support, $k_{\Delta 1}$.

Due to the reasons outlined above and considering that the initial model responses were already reasonably close to the experimental data, the model updating process was judged to require repetition using more refined settings to improve convergence and parameter estimation. Accordingly, Stage 2 of the model updating was re-run with all spring supports included as parameters, rather than limiting the update to the previously selected subset. The refined procedure incorporated the following adjustments.

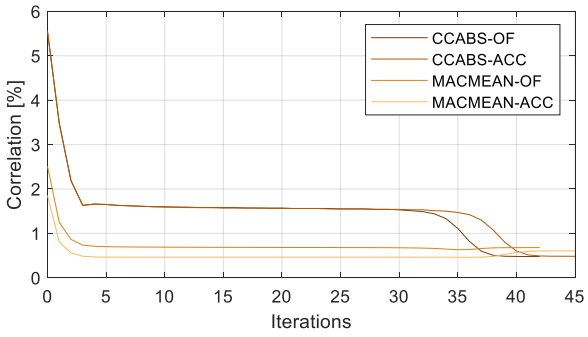
Error Function Criteria Adjustment: FEMTools evaluates model accuracy using a correlation coefficient based on the weighted relative differences between modal parameters. To better capture subtle improvements, the threshold for this coefficient, used as a convergence condition, was reduced from 1% to 0.1%, allowing the update to proceed through additional iterations with minor improvements.

Tighter Iteration Convergence Threshold: The criterion for the minimum relative improvement between consecutive iterations was also reduced from 0.1% to 0.001%, further enabling a more sensitive convergence process.

Increased Parameter Flexibility: The maximum allowable change in parameter values per iteration was increased to accommodate larger adjustments in spring stiffness values.

In summary, the revised Stage 2 procedure involved re-evaluating uncertainties in the support behaviour away from the pylon, informed by connection details and previous studies. This was followed by a series of manual stiffness adjustments, which indicated that further improvement was achievable. Finally, the process incorporated more refined FEMTools settings and convergence criteria, guided by insights from initial trial runs.

The revised model updating process converged after 45 iterations using accelerometry-based responses and 42 iterations using OF based responses. The progression of the correlation coefficient (CCABS) and the average weighted difference in Modal Assurance Criterion values (MACMEAN) throughout the iterations is illustrated in Figure 12.



436

437 Figure 12. Convergence of the iterative process during the second stage of FE model updating.

438 **3.2.3 FE model updating results**

439 Results of the FEMU are described in this section. As discussed in Section 3.2.2.1, during Stage 1 the modulus
440 of elasticity of the stay cables was selected as the parameter to be updated. As a result, the modulus of elasticity
441 value is updated to the value of 175 GPa.

442 The sensitivity results shown in Figure 7 and Figure 9 indicate that the tension forces were not sufficiently
443 sensitive for the update of the selected responses and were thus kept at their original values as reported by
444 Pakos et al. [33], as shown in Table 3.

445 Table 3. Initial and updated values of the stay cables' parameters.

	Stay cables' modulus of elasticity $E_{1\text{-}8}$ and $E_{9\text{-}12}$ [GPa]	**Post-tension forces for stay cable pairs [N]**					
		$F_{1\&2}$	**$F_{3\&4}$**	**$F_{5\&6}$**	**$F_{7\&8}$**	**$F_{9\&10}$**	**$F_{11\&12}$**
Initial model	140	229.7	72.4	16.3	21.1	563.6	328.5
Updating using OF	175	low sensitivity to model updating					
Updating using accelerometry	175	low sensitivity to model updating					

446

447 In Stage 2, the focus shifted to the support conditions. Table 4 presents the spring stiffness values before and
448 after updating. Significant changes were observed in all longitudinal springs (k_{Δ}) and in the rotational spring
449 at the deck–pylon connection ($k_{\phi 2}$). In contrast, the rotational spring at support 4 ($k_{\phi 4}$) remained virtually
450 unchanged, while $k_{\phi 1}$ and $k_{\phi 3}$ experienced only minor adjustments.

451

Table 4. Initial and updated values of spring stiffness at supports.

	Support 1		Support 2	Support 3		Support 4	
	k_Δ [N/m]	k_ϕ [Nm/rad]	k_ϕ [Nm/rad]	k_Δ [N/m]	k_ϕ [Nm/rad]	k_Δ [N/m]	k_ϕ [Nm/rad]
Initial model	6.00E+05	120	1.2E+02	6.00E+05	120	6.00E+05	120
OF updated model	4.24E+08	1575	1.6E+05	1.63E+09	132	3.03E+08	120
Accl. updated model	4.18E+08	1707	1.6E+05	1.62E+09	132	3.00E+08	120

Table 5 and Table 6 present the level of agreement between the modal responses of the initial and updated FE models and the experimental measurements obtained from accelerometry and OF systems. Overall, the updating process led to a substantial improvement in all identified natural frequencies. The most significant improvement, yet the least correlated, was observed for Mode 3, where the frequency errors were reduced from 16.00% and 15.98% to 1.42% and 1.41% for accelerometry and OF data, respectively. For Mode 4, the frequency was updated to match the experimental values exactly in both systems. Mode shape correlations also showed excellent agreement, with MAC values exceeding 99% across all modes. The comparison of the updated mode shapes with the experimental results is illustrated in Figure 13**.**

Table 5. Correlation of the modal data using the accelerometry based test results and the initial and the updated FE models.

	Modal frequency [Hz] (% error relative to data from accelerometry)			
Mode	**Accelerometry**	**Initial FE model**	**Update step 1**	**Update step 2**
1	5.1823	4.719 (-8.93)	5.026 (-3.02)	5.184 (0.02)
3	15.082	12.670 (-16.00)	13.505 (-10.46)	14.868 (-1.42)
4	19.178	18.161 (-5.31)	18.564 (-3.21)	19.178 (0.00)

	MAC [%]		
	Initial FE model	**Update step 1**	**Update step 2**
1	99.7	99.6	99.5
3	91.0	96.0	99.8

4	98.7	98.8	98.9

464

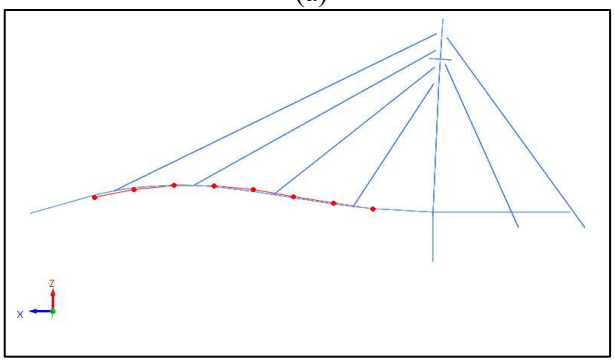
465 Table 6. Correlation of the modal data using the OF based test results and the initial and the updated FE
466 models.

	Modal frequency [Hz](% error relative to data from OF responses)			
Mode	**OF**	**Initial FE model**	**Update step 1**	**Update step 2**
1	5.177	4.719 (-8.85)	5.026 (-2.92)	5.179 (0.02)
3	15.080	12.670 (-15.98)	13.505 (-10.45)	14.868 (-1.41)
4	19.180	18.161 (-5.31)	18.564 (-3.21)	19.180 (0.00)

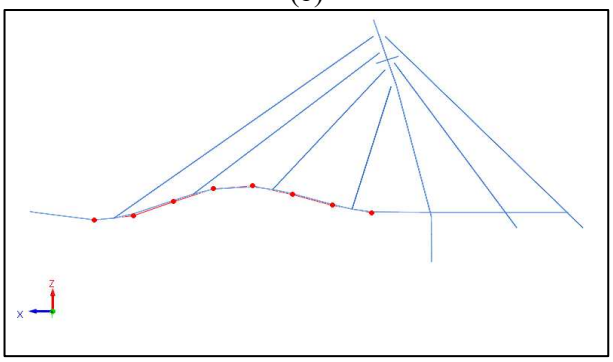
	MAC [%]		
	Initial FE model	**Update step 1**	**Update step 2**
1	99.7	99.5	99.5
3	89.1	94.3	99.5
4	98.4	98.7	99.0

467

(a)



(b)



(c)

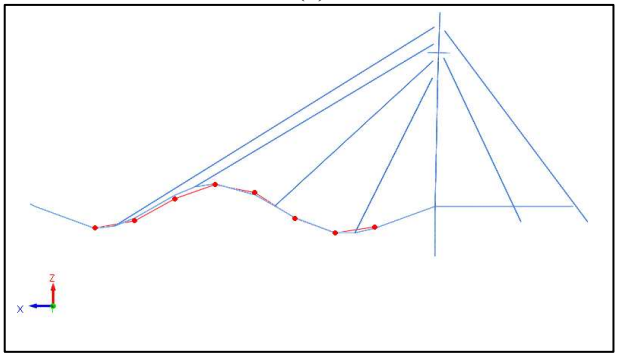


Figure 13 Comparison of the mode shapes from the final updated FE model (blue) and results obtained with measurements with OF (red) for (a) mode 1, (b) mode 3 and (c) mode 4.

The final updated models using the two measurement systems show a high degree of consistency. The largest discrepancy in natural frequencies between the accelerometry-based and OF-based models is observed for Mode 1, amounting to only 0.1% (see Table 7).

Table 7. Comparison of modal frequencies between the final updated FE models obtained with data from accelerometry and OF.

	Modal frequency [Hz]		
Mode	**Update using Accelerometry data**	**Update using OF data**	**Difference [%]**
1	5.184	5.179	0.096
3	14.868	14.868	0.000
4	19.178	19.180	0.010

4 Discussion

Although FE model updating, as implemented in commercial software packages, is typically an automated process, it should not be treated as a black-box procedure. Instead, careful consideration must be given to the selection of appropriate parameters and the specification of fit-for-purpose settings. Performing trial runs with varied initial values and convergence criteria, and structuring the updating in multiple stages, has been shown to improve the accuracy and reliability of the results [53–55]. For the current study, several additional trial runs were performed to verify the robustness of the selected parameters and the overall updating strategy. For example, when the stiffness values of the spring supports were updated while keeping the cable moduli of elasticity at their initial value (i.e. 140 GPa), effectively performing Stage 2 while skipping Stage 1, the model did not achieve the desired level of improvement. In this case, the frequency errors relative to the accelerometry and OF measurements were 1.4%, 9.2%, and 2.6% for Modes 1, 3, and 4, respectively. These findings underscore the importance of Stage 1, particularly the updating of the stay cables' modulus of elasticity.

The governing parameters affecting the effective stiffness of stay cables are the modulus of elasticity and the cross-sectional area, rather than the tensile forces [56]. A previous study by Shabbir and Omenzetter [36] using a genetic algorithm-based procedure found that the tension force in only one out of three pairs of cables within a tested full-scale footbridge had a significant influence on the model updating process. Supporting the present findings, the study by Pakos et al. [33] which examined the same bridge model analysed in this paper, concluded that certain variations in individual cable tension forces had minimal impact on the modal frequencies of both the deck and the pylon. For the current study, although Stage 2 concludes the main model updating process, an additional trial was conducted to verify whether further tuning of the cable post-tension forces, based on the final updated model, could yield further improvements. While sensitivity analysis indicated that adjustments to the tensions in cable pairs 1, 5 and 6 might be beneficial, subsequent updating confirmed that no further improvement in model performance was achieved. This outcome is likely attributable to the fact that the original tension values proposed by Pakos et al. [35] are already physically meaningful and consistent with the structural behaviour of the bridge.

The literature on a wide range of bridge types, including laboratory-scale bridge models, indicates that the error in modal frequencies between updated FE models and experimental measurements can range from 3% to 20%, or even higher in some cases [6,29,52,57,58]. In contrast, the updated FE models developed in the current study, based on both accelerometry and OF data, exhibited a maximum frequency error of only about 1.4% relative to the measurements. This level of accuracy suggests that the updated models provide a reliable representation of the actual structure. The high accuracy achieved can be attributed primarily to the simplicity of the scaled-down bridge model, which reduces the complexity typically encountered in full-scale structures. Furthermore, laboratory-based testing offers a controlled environment, effectively isolating the structure from operational and environmental factors that often introduce variability and reduce measurement precision in field applications.

Interoperability challenges present a major barrier to effectively connecting computational models with experimental data, particularly in the context of structural SHM. As Building Information Modelling (BIM) continues to gain prominence not only in design and construction but also in SHM applications, its ability to enable rapid and automated visualization of structural performance trends becomes increasingly valuable.

However, limited interoperability between BIM and FEM tools remains an open issue, as highlighted by O'Shea and Murphy [59]. Studies like Talebi et al. [60] suggest promising directions, such as MATLAB-based methodologies that facilitate automated data exchange between BIM and FEM systems for model updating using experimental input. In the current study, attempts to import a FEM from SAP2000 into FEMTools for sensitivity analysis were hindered by difficulties in recognising specific element types, such as links and cables. To overcome this, the SAP2000 Open Application Programming Interface (OAPI) was employed to enable two-way communication between SAP2000 and FEMTools, allowing all FEM analyses to be executed in SAP2000 while being managed through FEMTools [61].

5 Conclusions

The results of this study confirm that camera-based vibration monitoring can serve as a reliable tool for finite element (FE) model updating in structural dynamics applications. The following conclusions can be drawn from a detailed experimental and numerical investigation on a laboratory-scale cable-stayed bridge.

1. Non-contact vision measurements can achieve a level of accuracy comparable to traditional accelerometer-based systems. Among the two computer vision algorithms evaluated, the Optical Flow (OF) technique proved to be more robust and precise, yielding modal parameters that were in near-perfect agreement with accelerometer results. Frequency discrepancies were reduced to less than 0.1%, and Modal Assurance Criterion (MAC) values consistently exceeded 0.95, confirming the capability of vision-based systems to capture dynamic characteristics with high fidelity.

2. A sensitivity-driven, iterative model updating strategy that targets physically meaningful parameters, thus ensuring both numerical accuracy and interpretability, was validated. The staged updating procedure, i.e. first calibrating the cable stiffness and then refining boundary parameters, proved crucial for convergence and model stability. Any attempts to bypass the first stage by directly updating boundary conditions resulted in noticeably inferior agreement between the measurements and the FE model, highlighting the necessity of a sequential approach to the FE model calibration.

3. The final updated FE models, whether based on accelerometer or machine vision-derived data, achieved excellent correlation with experimental measurements, with modal frequency errors below 1.5%. This level of

agreement surpasses that reported in many comparable studies on bridge structures, reinforcing the potential of the proposed framework for accurate and physically interpretable FE model updating.

4. The findings suggest that machine vision-based techniques offer a practical, scalable, and non-intrusive alternative to conventional sensing systems, particularly suitable for scenarios where dense spatial coverage and/or minimal instrumentation are desired.

Despite its contributions, this study is subject to certain limitations. The investigation is conducted within a controlled laboratory environment and is primarily focused on the deck response, which may not fully capture the complexity and variability of full-scale bridge behaviour under real operational and environmental conditions. Moreover, the current framework does not yet exploit the full capability of computer vision systems to simultaneously monitor other critical components, such as cables and pylons. Nevertheless, the proposed approach provides a solid foundation for extending vision-based finite element (FE) updating methodologies to real-world bridge applications. Future research should aim to overcome these limitations by incorporating multi-camera systems for comprehensive three-dimensional motion capture, enabling the monitoring of entire bridge systems. Further developments in automation through data-driven and machine learning techniques, as well as integration with Building Information Modelling (BIM) platforms, will be essential to achieve real-time, automated model calibration and advance next-generation structural health monitoring solutions.

References

1. Jaishi, B.; Ren, W.-X. Structural Finite Element Model Updating Using Ambient Vibration Test Results. **2005**, doi:10.1061/ASCE0733-94452005131:4617.
2. Hu, J.; Lam, H.F.; Yang, J.H. Operational Modal Identification and Finite Element Model Updating of a Coupled Building Following Bayesian Approach. *Struct. Control Health Monit.* **2018**, *25*, doi:10.1002/stc.2089.
3. Mottershead, J.E. Model Updating in Structural Dynamics: A Survey. *J. Sound Vib.* **1993**, *2*, 347–375.
4. Brownjohn, J.; Xia, P.-Q.; Hao, H.; Xia, Y. *Civil Structure Condition Assessment by FE Model Updating: Methodology and Case Studies*; 2001; Vol. 37;.
5. Chung, T.T.; Cho, S.; Yun, C.B.; Sohn, H. Finite Element Model Updating of Canton Tower Using Regularization Technique. *Smart Struct. Syst.* **2012**, *10*, 459–470, doi:10.12989/sss.2012.10.4_5.459.
6. Ding, Y.; Li, A. Finite Element Model Updating for the Runyang Cable-Stayed Bridge Tower Using Ambient Vibration Test Results. *Advances in Structural Engineering 11*, doi:https://doi.org/10.1260/136943308785082599.

7. Domaneschi, M.; Zamani Noori, A.; Pietropinto, M.V.; Cimellaro, G.P. Seismic Vulnerability Assessment of Existing School Buildings. *Comput. Struct.* **2021**, *248*, doi:10.1016/j.compstruc.2021.106522.

8. Moaveni, B.; Conte, J.P.; Hemez, F.M. Uncertainty and Sensitivity Analysis of Damage Identification Results Obtained Using Finite Element Model Updating. *Computer-Aided Civil and Infrastructure Engineering* **2009**, *24*, 320–334, doi:10.1111/j.1467-8667.2008.00589.x.

9. Brownjohn, J.M.W.; Xia, P.-Q. Dynamic Assessment of Curved Cable-Stayed Bridge by Model Updating. *Journal of Structural Engineering* **2000**, *126*, 252–260, doi:10.1061/(asce)0733-9445(2000)126:2(252).

10. Shabbir, F.; Omenzetter, P. Model Updating Using Genetic Algorithms with Sequential Niche Technique. *Eng. Struct.* **2016**, *120*, 166–182, doi:10.1016/j.engstruct.2016.04.028.

11. Asgari B.; Osman S. A.; Adnan A. Sensitivity Analysis of the Influence of Structural Parameters on Dynamic Behaviour of Highly Redundant Cable-Stayed Bridges. *Advances in Civil Engineering* **2013**, doi:https://doi.org/10.1155/2013/426932.

12. Vasallo Belver, A.; Zivanovic, S.; Dang, H.; Istrate, M.; Iban, A.L. Modal Testing and FE Model Updating of a Lively Staircase Structure. In Proceedings of the Proceedings of the SEM IMAC XXX Conference; Society for Experimental Mechanics Inc., 2012.

13. Ghannadi, P.; Kourehli, S.S. Model Updating and Damage Detection in Multi-Story Shear Frames Using Salp Swarm Algorithm. *Earthquake and Structures* **2019**, *17*, 63–73, doi:10.12989/eas.2019.17.1.063.

14. Zapico, J.L.; González, M.P.; Friswell, M.I.; Taylor, C.A.; Crewe, A.J. Finite Element Model Updating of a Small Scale Bridge. *J. Sound Vib.* **2003**, *268*, 993–1012, doi:10.1016/S0022-460X(03)00409-7.

15. Xu, Y.; Brownjohn, J.M.W. Review of Machine-Vision Based Methodologies for Displacement Measurement in Civil Structures. *J. Civ. Struct. Health Monit.* **2018**, *8*, 91–110, doi:10.1007/s13349-017-0261-4.

16. Luo, K.; Kong, X.; Zhang, J.; Hu, J.; Li, J.; Tang, H. Computer Vision-Based Bridge Inspection and Monitoring: A Review. *Sensors* **2023**, *23*, doi:10.3390/s23187863.

17. Payawal, J.M.G.; Kim, D.K. Image-Based Structural Health Monitoring: A Systematic Review. *Applied Sciences (Switzerland)* **2023**, *13*, doi:10.3390/app13020968.

18. Panigati, T.; Abbozzo, A.; Pace, M.A.; Temur, E.; Cigan, F.; Kromanis, R. Dynamic Identification of Bridges Using Multiple Synchronized Cameras and Computer Vision. *Infrastructures (Basel).* **2025**, *10*, doi:10.3390/infrastructures10020037.

19. Yan, Z.; Jin, Z.; Teng, S.; Chen, G.; Bassir, D. Measurement of Bridge Vibration by UAVs Combined with CNN and KLT Optical-Flow Method. *Applied Sciences (Switzerland)* **2022**, *12*, doi:10.3390/app12105181.

20. Bolognini, M.; Izzo, G.; Marchisotti, D.; Fagiano, L.; Limongelli, M.P.; Zappa, E. Vision-Based Modal Analysis of Built Environment Structures with Multiple Drones. *Autom. Constr.* **2022**, *143*, doi:10.1016/j.autcon.2022.104550.

21. Panigati, T.; Zini, M.; Striccoli, D.; Giordano, P.F.; Tonelli, D.; Limongelli, M.P.; Zonta, D. Drone-Based Bridge Inspections: Current Practices and Future Directions. *Autom. Constr.* **2025**, *173*, doi:10.1016/j.autcon.2025.106101.

22. Kromanis, R.; Xu, Y.; Lydon, D.; Martinez del Rincon, J.; Al-Habaibeh, A. Measuring Structural Deformations in the Laboratory Environment Using Smartphones. *Front. Built Environ.* **2019**, *5*, doi:10.3389/fbuil.2019.00044.

23. Zhao, X.; Ri, K.; Wang, N. Experimental Verification for Cable Force Estimation Using Handheld Shooting of Smartphones. *J. Sens.* **2017**, *2017*, doi:10.1155/2017/5625396.

24. Kalybek, M.; Bocian, M.; Nikitas, N. Performance of Optical Structural Vibration Monitoring Systems in Experimental Modal Analysis. *Sensors (Switzerland)* **2021**, *21*, 1–24, doi:10.3390/s21041239.

25. Kalybek, M.; Bocian, M.; Pakos, W.; Grosel, J.; Nikitas, N. Performance of Camera-Based Vibration Monitoring Systems in Input-Output Modal Identification Using Shaker Excitation. *Remote Sens. (Basel).* **2021**, *13*, doi:10.3390/rs13173471.

26. Dong, C.Z.; Celik, O.; Catbas, F.N. Marker-Free Monitoring of Thegrandstand Structures and Modalidentification Using Computer Vision Methods. *Struct. Health Monit.* **2019**, *5–6*, 1491–1509, doi:https://doi.org/10.1177/1475921718806.

27. Bocian, M.; Nikitas, N.; Kalybek, M.; Kużawa, M.; Hawryszków, P.; Bień, J.; Onysyk, J.; Biliszczuk, J. Dynamic Performance Verification of the Rędziński Bridge Using Portable Camera-Based Vibration Monitoring Systems. *Archives of Civil and Mechanical Engineering* **2023**, *23*, doi:10.1007/s43452-022-00582-7.

28. Dong, C.Z.; Bas, S.; Catbas, F.N. Investigation of Vibration Serviceability of a Footbridge Using Computer Vision-Based Methods. *Eng. Struct.* **2020**, *224*, doi:10.1016/j.engstruct.2020.111224.

29. Park, G.; Hong, K.N.; Yoon, H. Vision-Based Structural Fe Model Updating Using Genetic Algorithm. *Applied Sciences (Switzerland)* **2021**, *11*, 1–16, doi:10.3390/app11041622.

30. Shu, J.; Zhang, C.; Chen, X.; Niu, Y. Model-Informed Deep Learning Strategy with Vision Measurement for Damage Identification of Truss Structures. *Mech. Syst. Signal Process.* **2023**, *196*, doi:10.1016/j.ymssp.2023.110327.

31. Mottershead, J.E.; Link, M.; Friswell, M.I. The Sensitivity Method in Finite Element Model Updating: A Tutorial. *Mech. Syst. Signal Process.* **2011**, *25*, 2275–2296, doi:10.1016/j.ymssp.2010.10.012.

32. Živanović, S.; Pavic, A.; Reynolds, P. Finite Element Modelling and Updating of a Lively Footbridge: The Complete Process. *J. Sound Vib.* **2007**, *301*, 126–145, doi:10.1016/j.jsv.2006.09.024.

33. Pakos, W.; Wójcicki, Z.; Grosel, J.; Majcher, K.; Sawicki, W. Experimental Research of Cable Tension Tuning of a Scaled Model of Cable Stayed Bridge. *Archives of Civil and Mechanical Engineering* **2016**, *16*, 41–52, doi:10.1016/j.acme.2015.09.001.

34. *CSi Analysis Reference Manual*; Computers & Structures, Inc., 2013;

35. Pakos, W. The experimental and theoretical analysis of active elimination of cables vibration in cable stayed footbridges. *Wrocław University of Science and Technology (PhD Thesis)* **2012**.

36. Shabbir, F.; Omenzetter, P. Model Updating Using Genetic Algorithms with Sequential Niche Technique. *Eng. Struct.* **2016**, *120*, 166–182, doi:10.1016/j.engstruct.2016.04.028.

37. Bradski, G.R..; Kaehler, Adrian. *Learning OpenCV : Computer Vision with the OpenCV Library*; O'Reilly, 2008; ISBN 9780596516130.

38. Xu, Y.; Brownjohn, J.; Kong, D. A Non-Contact Vision-Based System for Multipoint Displacement Monitoring in a Cable-Stayed Footbridge. *Struct. Control Health Monit.* **2018**, *25*, doi:10.1002/stc.2155.

39. Xiao, P.; Wu, Z.Y.; Christenson, R.; Lobo-Aguilar, S. Development of Video Analytics with Template Matching Methods for Using Camera as Sensor and Application to Highway Bridge Structural Health Monitoring. *J. Civ. Struct. Health Monit.* **2020**, *10*, 405–424, doi:10.1007/s13349-020-00392-6.

40. Feng, D.; Feng, M.Q.; Ozer, E.; Fukuda, Y. A Vision-Based Sensor for Noncontact Structural Displacement Measurement. *Sensors (Switzerland)* **2015**, *15*, 16557–16575, doi:10.3390/s150716557.

41. Xu, Y.; Zhang, J.; Brownjohn, J. An Accurate and Distraction-Free Vision-Based Structural Displacement Measurement Method Integrating Siamese Network Based Tracker and Correlation-Based Template Matching. *Measurement (Lond).* **2021**, *179*, doi:10.1016/j.measurement.2021.109506.

42. Bai, Y.; Sezen, H.; Yilmaz, A.; Qin, R. Bridge Vibration Measurements Using Different Camera Placements and Techniques of Computer Vision and Deep Learning. *Advances in Bridge Engineering* **2023**, *4*, doi:10.1186/s43251-023-00105-1.

43. Pan, B.; Qian, K.; Xie, H.; Asundi, A. Two-Dimensional Digital Image Correlation for in-Plane Displacement and Strain Measurement: A Review. *Meas. Sci. Technol.* **2009**, *20*, doi:10.1088/0957-0233/20/6/062001.

44. Hacıefendioğlu, K.; Kahya, V.; Limongelli, M.G.; Okur, F.Y.; Altunışık, A.C.; Aslan, T.; Pembeoğlu, S.; Duman, C.; Bostan, A.; Aleit, H. Applications of Optical Flow Methods and Computer Vision in Structural Health Monitoring for Enhanced Modal Identification. *Structures* **2024**, *69*, doi:10.1016/j.istruc.2024.107414.

45. Lucas, B.D.; Kanade, T. An Iterative Image Registration Technique with an Application to Stereo Vision (IJCAI) An Iterative Image Registration Technique with an Application to Stereo Vision. In Proceedings of the Proceedings of Imaging Understanding Workshop; 1981; pp. 121–130.

46. Shi Jianbo; Tomasi Carlo Good Features to Track. In Proceedings of the Proceedings of the IEEE Computer Society Conference on Computer Vision and Pattern Recognition; IEEE conference on computer vision and pattern recognition, 1994; pp. 593–600.

47. Pakos, W.; Grosel, J. Reduction of Cable Vibrations in a Cable Stayed Bridge under Biharmonic Excitation. *Eng. Struct.* **2019**, *189*, 1–10, doi:10.1016/j.engstruct.2019.03.054.

48. EFMETAL - Ropes Available online: http://www.efmetal.com.pl/en/html/liny.php?cat=l6 (accessed on 5 May 2026).

49. *FEMtools Model Updating User's Guide*; Dynamic Design Solutions (DDS) NV: Leuven, Belgium, 2012;

50. *ANSYS Interface and Driver User ' s Guide*; Dynamic Design Solutions (DDS) NV, 2021;

51. Živanović, S.; Pavic, A.; Reynolds, P. Finite Element Modelling and Updating of a Lively Footbridge: The Complete Process. *J. Sound Vib.* **2007**, *301*, 126–145, doi:10.1016/j.jsv.2006.09.024.

52. Shabbir, F.; Omenzetter, P. Model Updating Using Genetic Algorithms with Sequential Niche Technique. *Eng. Struct.* **2016**, *120*, 166–182, doi:10.1016/j.engstruct.2016.04.028.

53. Turek, M.; Ventura, C.E.; Dascotte, E. Model Updating of the Ironworkers Memorial Second Narrows Bridge, Vancouver, Canada. In Proceedings of the Society for Experimental Mechanics Series; 2011; Vol. 5, pp. 49–56.

54. Petersen, W.; Øiseth, O. Sensitivity-Based Finite Element Model Updating of a Pontoon Bridge. *Eng. Struct.* **2017**, *150*, 573–584, doi:10.1016/j.engstruct.2017.07.025.

693 55. Lakzaeian, F.H. Ambient Vibration Testing and Finite Element Model Updating of a Concrete
694 Footbridge. In Proceedings of the 4th International Operational Modal Analysis Conference, IOMAC
695 2011; 2011; pp. 403–411.

696 56. Nazmy, A.S.; Abdel-Ghaffar, A.M. Three-Dimensional Nonlinear Static Analysis of Cable-Stayed
697 Bridges. *Comput. Struct.* **1990**, *34*, 257–271.

698 57. Svendsen, B.T.; Petersen, Ø.W.; Frøseth, G.T.; Rønnquist, A. Improved Finite Element Model
699 Updating of a Full-Scale Steel Bridge Using Sensitivity Analysis. *Structure and Infrastructure*
700 *Engineering* **2022**, *19*, 315–331, doi:10.1080/15732479.2021.1944227.

701 58. Jung, D.S.; Kim, C.Y. Finite Element Model Updating on Small-Scale Bridge Model Using the Hybrid
702 Genetic Algorithm. *Structure and Infrastructure Engineering* **2013**, *9*, 481–495,
703 doi:10.1080/15732479.2011.564635.

704 59. O'Shea, M.; Murphy, J. Design of a BIM Integrated Structural Health Monitoring System for a Historic
705 Offshore Lighthouse. *Buildings* **2020**, *10*, doi:10.3390/BUILDINGS10070131.

706 60. Talebi, A.; Potenza, F.; Gattulli, V. Interoperability between BIM and FEM for Vibration-Based Model
707 Updating of a Pedestrian Bridge. *Structures* **2023**, *53*, 1092–1107, doi:10.1016/j.istruc.2023.04.115.

708 61. Dynamic Design Solutions NV (DDS) *SAP2000 Interface and Driver User's Guide*; 2021;

709